



Design and Real Time Digital Simulator Implementation of a Takagi Sugeno Fuzzy Controller for Battery Management in Photovoltaic Energy System Application

A. Basu*, M. Singh

Department of Electrical Engineering, National Institute of Technology, Jamshedpur, India

PAPER INFO

Paper history:

Received 21 September 2021

Received in revised form 22 June 2022

Accepted 28 July 2022

Keywords:

Photovoltaic Energy Storage System

Bi-directional Converter

Takagi Sugeno Fuzzy Controller

RT-LAB

ABSTRACT

This paper presents a comprehensive design and control strategy for a photovoltaic (PV) energy storage system. The system consists of a 2kW photovoltaic system, two converter circuits, a resistive load of 6 Ohm and a lithium-ion battery storage integrated with DC Bus applying constant power to the resistive load. This scheme offered two converter topologies, one is a boost converter and another is a DC/DC bidirectional converter. The boost converter is directly connected in series to the PV array whereas the bidirectional DC/DC converter (BDC) is connected to the battery. The boost converter is used to regulate the maximum power point tracking (MPPT) of the PV array. Closed-loop control of the bidirectional controller is implemented with Takagi-Sugeno Fuzzy (TS-Fuzzy) controller to regulate the battery charging and discharging power flow. The proposed scheme provides a good stabilization in the DC bus voltage. Simulation results of the proposed control schema under MATLAB/Simulink are presented and compared with the Proportional Integral (PI) controller. The simulation results obtained from MATLAB are verified on Real Time Digital Simulator (RTDS).

doi: 10.5829/ije.2022.35.12c.01

NOMENCLATURE

I_{pv}	Current from PV cell in amps	V_{oc}	Open-Circuit voltage of PV array in volts
I_O	Reverse saturation current of diode in amps	I_{sc}	Short circuit current of PV array in amps
η	Diode ideality factor	L	Inductor of boost converter in henry
V	Voltage across diode in volts	I_o	Output current of boost converter in amps
V_T	Thermal voltage in volts	C_2	Output capacitor of boost converter in farads
V_{mp}	Voltage of PV array at MPP in volts	ΔI_L	Ripple current of bidirectional converter
I_{mp}	Current of PV at MPP in amps	V_O	Output voltage of boost converter in volts
F_{sw}	Switching frequency in kHz	V_{bat}	Battery voltage in volts
ΔV	Output voltage ripple of boost converter	ΔV_{dc}	Ripple voltage of bidirectional converter
Δi_i	Output current ripple of boost converter	V_{dc}	Voltage of DC bus in volts
D	Duty cycle	ΔI_L	Ripple current of bidirectional converter
V_{in}	Input voltage of boost converter in volts	I_{bat}	Battery current in amps

1. INTRODUCTION

Sustainable energy has played a vital role to control the global emission. Over the last few decades on average, 300GW renewable energy sources (RES) were grown in the year between 2018 and to reach the goal of the Paris agreement, according to the IEA'S Sustainable

Development Scenario (SDC). A country like India has a significant advantages as there is a huge potential for sustainable energy resources. In 2023, the installed renewable energy capacity will be account for 35% [1]. The installed capacity of renewable energy in India is about 150GW in which wind power is 40.08GW, 49.34GW solar power, 10.61GW bio power, 4.83GW

*Corresponding Author Institutional Email: 2020rsee004@nitjsr.ac.in
(A. Basu)

small hydro and 46.51 GW large hydro. The Government of India has targeted to expand the renewable energy installed capacity to 500 GW by 2030². Photovoltaic power plays a significant role in power generation and has become essential due to the storage and the environmental impact. PV system is a non-linear system, hence it is too sensitive to determine the characteristics of the magnitude of the systems, which have the single point where the power is maximum. Faranda et al. [2] discussed that the power produced by the PV is more than 45%. Berrera et al. [3] discussed that the PV generation system has two problems i.e., the energy conversion efficiency is low due to the weather changes and hence the power generation of solar array is changed. Liu et al. [4] proposed that the PV array consists of non-linear characteristics, hence the I-V and P-V characteristics are always changing with weather conditions. Eswam et al. [5] proposed the P&O method for the MPPT technique irrespective of different irradiation and temperature. Eswam et al. [5] also proposed another method of MPPT i.e., the incremental conductance method (INC). The comparison of different types of technique in MPPT such as fuzzy controller, neural network, current sweep etc. is discussed in the literature [6-8]. The integration of the PV with the energy storage system (ESS) is an emerging research area. Usually, ESS is constituted by battery. However, the loads are also necessary when PV and battery storage system (BSS) are connected. Samadi and Saif [9, 10] presented the mathematical model for state-of-charging (SOC) estimation for battery management system. However, the performance of the controller in the presence of a non-linear system is not discussed. Based on the literature review, various control algorithms are proposed for the battery management system [11]. The proposed TS-fuzzy control algorithm is compared to the Proportional Integral (PI) control algorithm. The conventional PI controller gains value are fixed for the certain radiation and load. Any change in these values the controller output signal will not be appropriate [12, 13]. Moreover, PI controller has higher overshoot and undershoot values, which is reduced by the proposed controller. The performance of the controller is analyzed in terms of battery current, load current and settling time. In this paper, a circuitry modelling and control strategy of a 2kW PV energy storage system is presented. The PV array directly converts the sunlight into an electrical signal (DC). The DC output of the PV array is given to the boost converter to implement the MPPT. The maximum power is extracted by using Perturb & Observe (P&O) method. A 48 Volts, 200Ah lithium-ion battery is used for the energy storage system. Moreover, the simulation results show the performance parameter of the TS-Fuzzy controller.

2. PHOTOVOLTAIC ENERGY STORAGE SYSTEM

The proposed photovoltaic (PV) energy system is shown in Figure 1. The system is composed of a photovoltaic cell; a boost converter performs MPPT technique of a PV array through P&O algorithm, a 48V battery storage, connected through a bidirectional DC-DC converter. Some authors have proposed a classical controller scheme for the control mechanism of a bidirectional DC/DC converter. Though classical controllers have the advantage of non-zero steady-state error but also have the limitations associated with overshoot, undershoot, high settling time etc. [14]. Given the ongoing limitations, this paper proposes a sophisticated design of Takagi-Sugeno Fuzzy controller scheme.

2.1. Modelling of Pv Cell The equivalent circuit topology of a PV model is shown in Figure 2.

The PV current (I_{pv}) is given by Equation (1) [15, 16].

$$I_{pv} = I_D + I \tag{1}$$

$$I_{pv} = I_0 \left(e^{\frac{V}{nV_T}} - 1 \right) \tag{2}$$

$$\text{Since, } I_D = I_0 \left(e^{\frac{V}{nV_T}} - 1 \right) \tag{3}$$

$$I = I_{pv} = I_0 \left(e^{\frac{V}{nV_T}} - 1 \right) \tag{4}$$

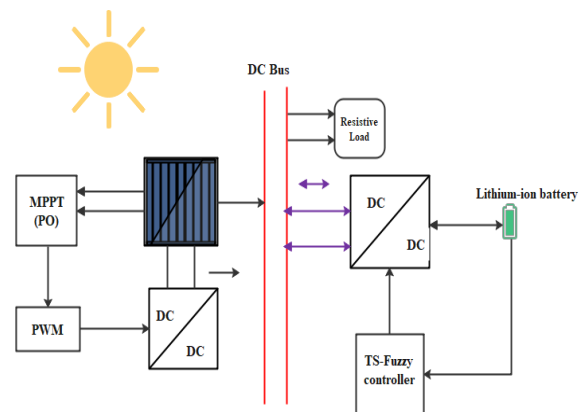


Figure 1. Schematic diagram of photovoltaic Energy System

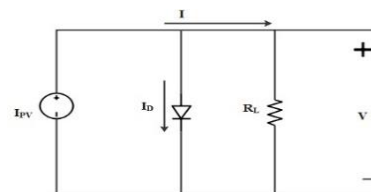


Figure 2. Electrical circuit model of PV panels

² <https://www.investindia.gov.in/sector/renewable-energy>

where I_D represents the diode current depends upon voltage and temperature. Using the above equations, the PV array is modeled in MATLAB, from the data sheet of 1Soltech 1STH-215-P with a specified temperature of 25° C. The power –voltage curve of PV panel with different irradiation values is presented in Figure 3.

The parameters of the proposed PV system are shown in Table 1.

2. 2. Design of Boost Converter

Figure 4 represents the circuit diagram of a boost converter used in this system. The switching frequency (F_{sw}) is considered as 5 kHz and the output voltage ripple (ΔV) and output current ripple (Δi_i) are considered as 5% and 10 %, respectively.

The design parameters of the boost converter are shown below [17]:

$$\text{Duty Cycle}(D)=1-(V_{in}/V_o) \tag{5}$$

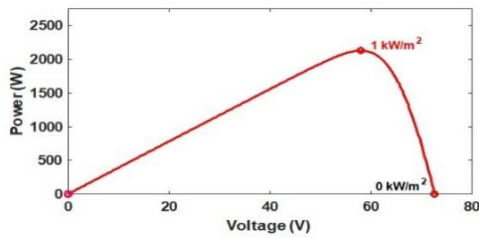


Figure 3. Power-voltage curve at the irradiation of 1000W/m² and 0W/m²

TABLE 1. Parameters of proposed PV array

Parameters	Values
PV array	5 parallel string 2 series connected module per string Total=2kWp
PV array Open circuit voltage (Voc)	36.3 V
PV array Voltage at maximum power point (Vmp)	29V
PV array Short circuit current (Isc)	7.84A
PV array Current at maximum power point (Imp)	7.35A

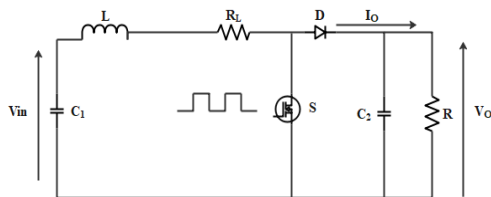


Figure 4. Boost converter Topology

V_{in} = input of boost converter=output of PV array.
The inductor value is given as,

$$L=V_{in} D/(2\Delta i_i F_{sw}) \tag{6}$$

The output capacitor value is given by,

$$C_2=I_{O}D/(\Delta V F_{sw}) \tag{7}$$

The parameters of the boost converter are illustrated in Table 2.

3. MAXIMUM POWER POINT TRACKER

The MPPT with PWM control method measure the current and voltage of the PV array and generates the duty cycle for the converter. Due to simplicity, ease of application, periodic tuning is not required and is used in both analogue and digital domains Perturb & Observation (P&O) is preferred for maximum power point tracking (MPPT) [18].

The basic control actions for various operation points in the P&O method are shown in the Table 3.

4. BI-DIRECTIONAL DC/DC CONVERTER

The bidirectional converters allow transferring of power of two DC sources in either direction. The converter consists of two switches S_{buck} and S_{boost} , which manages the charging –discharging process as shown in Figure 5.

In the buck mode switch S_{buck} in on, stored energy in the inductor is supplied to the battery for charging purposes. For operation in buck mode, the inductor filter design is carried out as follows:

$$L_+ = \frac{(V_{dc}-V_{bat})D_+}{\Delta I_L f_{sw}} \tag{8}$$

TABLE 2. Parameters of boost converter

Parameters	Values
Input voltage of boost converter	50-52 Volts
output voltage of boost converter	60 Volts
Duty Cycle	0.15-0.75
inductance	1.7 mH
Output capacitance	1.786 μF

TABLE 3. Various control operation of P&O Algorithm

Case	ΔV	ΔP	Voltage Control Action	Duty Cycle
1	+	+	Increase V by ΔV	Decrease
2	-	-	Increase V by ΔV	Decrease
3	-	+	Decrease V by ΔV	Increase
4	+	-	Decrease V by ΔV	Increase

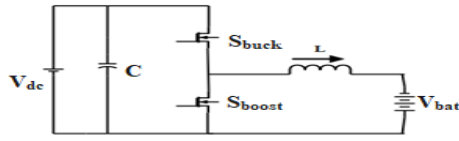


Figure 5. DC/DC non-isolated bi-directional converter

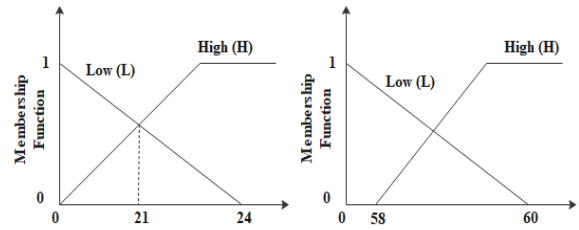


Figure 6. Membership function of TS-Fuzzy control

$$C_+ = \frac{(1-D_+)V_{bat}}{8L+\Delta V_{bat}f^2} \tag{9}$$

where, ΔI_L and f_{sw} are the ripple current and switching frequency of the buck converter respectively. In the boost mode switch S_{boost} is on, inductor discharges the stored energy. For bidirectional converter operation in the boost mode, the inductor filter design value is carried out as follows:

$$L_- = \frac{V_{bat} D_-}{\Delta I_L f_{sw}} \tag{10}$$

$$C_- = \frac{V_{dc} D_-}{R_0 \Delta V_{dc} f_{sw}} \tag{11}$$

ΔV_{dc} , is the ripple voltage of the boost converter respectively. The parameters of the bidirectional converter are illustrated in Table 4.

5. BATTERY MANAGEMENT SYSTEM

To charge the battery bank, which is connected to the PV array as the energy storage system (ESS) battery management system (BMS) is used. The charging-discharging of the ESS depends on the power generated by the PV array [19]. If the total power is greater than the desired limit, the battery is charging or vice-versa. The initial state of charge (SOC %) of the battery is considered 80%. Here, TS-fuzzy logic controller is used for BMS.

The Takagi-Sugeno model is considered as an exact representation of the non-linear system. In general, there are two approaches for designing the TS-fuzzy model.

1. Identify the input-output data for the system.
2. Derivation from the given non-linear system.

In this system, load voltage (V_c)/current (i_L) are taken as input variables for designing the TS-fuzzy controller. Input signals are fuzzified by means of two linguistic memberships (MFs) values; L and H for low and high respectively as shown in Figure 6.

TABLE 4. Parameters of bidirectional converter

Parameters	Values
C	500 μF
L	1 mH
f_{sw}	5kHz

Here we choose a nonlinear term: i_L
 Because the average current is about 21 A
 Therefore, we define the range: 0-24

$$\begin{cases} M_{11}(i_L(t)) = \frac{1}{24} i_L(t) \\ M_{12}(i_L(t)) = 1 - \frac{1}{24} i_L(t) \end{cases} \tag{12}$$

The model rule i (Buck Mode):

If $q_1(t)$ is M_{i1}

Then,

$$\dot{x}(t) = A_i x(t) + B_i u(t) + E_i v(t), i = 1,2 \tag{13}$$

where, $q_1(t)$: The non linear term

M_{i1} : The i th Membership function

Control Rule i (Buck Mode):

If $q_1(t)$ is M_{i1}

Then $u(t) = F_i x(t), i = 1,2$

where, $F_i =$ Control gain

The closed loop TS-Fuzzy control signal (Buck Mode):

$$\dot{x}(t) = \sum_{i=1}^2 \sum_{j=1}^2 h_i(q(t)) h_j(q(t)) (A_i - B_i F_j) x(t) + E_i v(t) \tag{14}$$

Another nonlinear term: V_c

Because the average DC bus voltage is about 58 V

So we define the range: 0-60

$$\begin{cases} M_{21}(V_c(t)) = \frac{1}{60} V_c(t) \\ M_{22}(V_c(t)) = 1 - \frac{1}{60} V_c(t) \end{cases} \tag{15}$$

Model Rule i (Boost Mode);

If, $q_1(t)$ is M_{P1} , $q_2(t)$ is M_{P2}

Then,

$$\dot{x}(t) = A_i x(t) + B_i u(t) + E_i v(t), i = 1,2,4 \tag{16}$$

where, $q_1(t), q_2(t)$: The non linear term

M_{P1}, M_{P2} : The i th Membership function

Control Rule i (Boost Mode):

If, $q_1(t)$ is $M_{P1}, q_2(t)$ is M_{P2}

Then, $u(t) = -F_i x(t), i = 1,2,4$

where, $F_i =$ Control gain

The closed loop TS-Fuzzy control signal (Boost Mode):

$$\dot{x}(t) = \sum_{i=1}^4 \sum_{j=1}^4 h_i(q(t)) h_j(q(t)) (A_i - B_i F_j) x(t) + E_i v(t) \tag{17}$$

6. RTDS IMPLEMENTATION AND RESULT DISCUSSION

The real time simulator is powerful modulator, distributed real time simulator, implemented on MATLAB/Simulink model-based design using in hardware-in-loop and off-line simulation. The architecture of RT-LAB is shown in the Figure 7.

It consists of host and target. The host is a Personal Computer in which MATLAB and RT-LAB are loaded. The target machine includes Intel Xeon E3 V5 CPU, Kintex-7 FPGA, 325T, 326,000 logic cells, and 840 DSP slice. The TCP/IP connects target machine and the host computer. The host PC interfaces and communicates with the target through Ethernet. Digital Storage Oscilloscope is used for data observation and verification of real simulation. According to the RT-LAB naming convention, the subsystems are named with a prefix which identifying their function. The prefixes are described as SM_main subsystem (always one). It contains the computational elements of the model. In this scheme, blocks namely PV model, boost converter, bidirectional converter, battery and load are assembled to construct SM_main subsystem (Figure 8). SC_main subsystem (at most one): In general, it includes all user interface blocks. In this scheme, blocks namely scope and manual switches are used as shown in Figure 9.

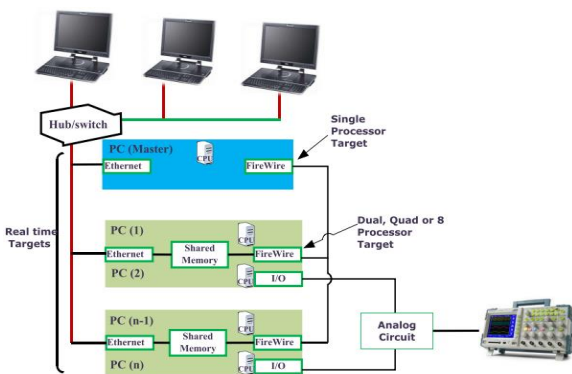


Figure 7. RT-LAB Simulator architecture

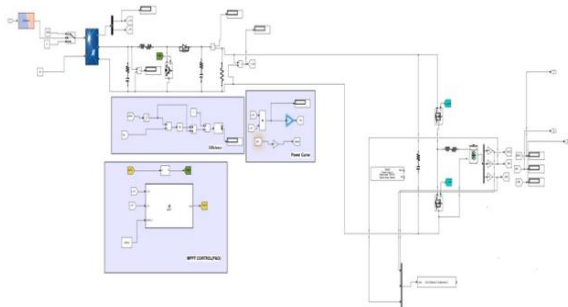


Figure 8. Configuration of the SM_main subsystem

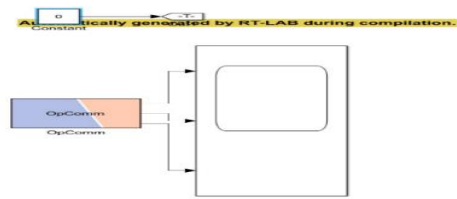


Figure 9. Configuration of the SC_main subsystem

The step size of the simulation is 0.02 ms. Firstly, the closed loop control of the bidirectional converter is implemented in the RT-LAB by using PI Controller. Then the proposed TS-Fuzzy controller is implemented to modify the performance of the parameter.

The real time results of PI controller are shown in Figure 10. It is demonstrated in Figure10 (a) that when the solar isolation is 1000W/m², the battery is charging. With a decrease in solar isolation there is a decreased in the produced power and the battery goes discharging. In the discharging mode, the battery current (*I_{bat}*) flows in reverse direction shown in Figure 10(c). An overshoot is observed during charging mode in case of PI controller.

The overshoot is eliminated in TS-Fuzzy controller. Remarkable ripple in battery current is found with PI but with TS-Fuzzy controller, it is eliminated shown in Figure 11(d).

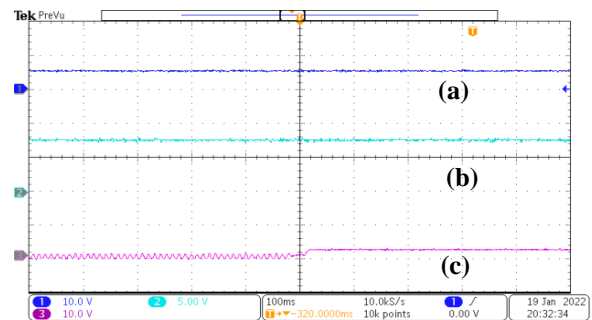


Figure 10. RTDS Hardware results for PI Controller (top to bottom) (a) SOC (20V/div), (b) V_{bat} (10V/div), (c) I_{bat} (5V/div)

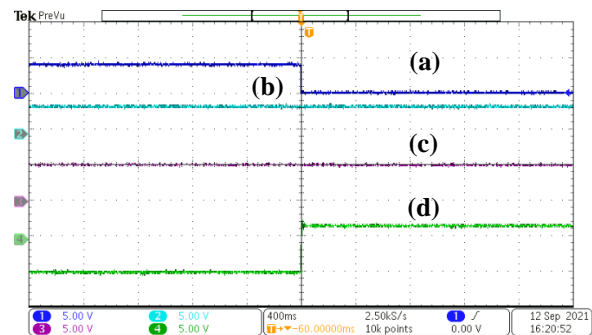


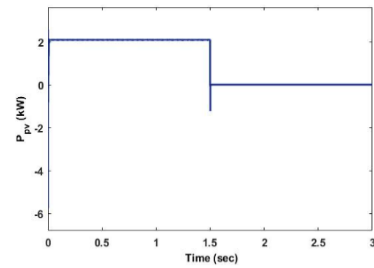
Figure 11. RTDS Hardware results for TS-fuzzy controller (top to bottom) (a) irr (250V/div), (b) SOC (20V/div), (c) V_{bat} (10V/div), (d) I_{bat} (5V/div)

7. SIMULATION RESULTS

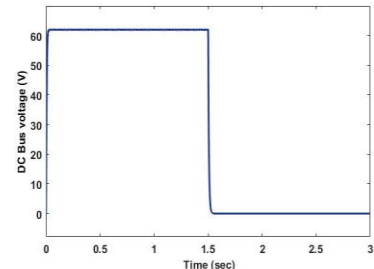
Simulated results of the PV system are shown in Figure 12. Figure 12(a) shows that at $t=0$ to $1.5s$, the irradiation is $1000W/m^2$, output voltage of PV array is $60V$ and the current is $40A$. At $t=1.5s$ to $3s$ the irradiation decreases at $0 W/m^2$, the voltage and current of the PV array decreases $0V$ and $0A$ respectively are shown in Figures 12(b) and 12(c). The DC bus voltage maintain the constant voltage around 60 Volts as shown in Figure 12(d). Meanwhile, from Figure 10(e) it observes that the system can track the maximum power of $2kW$ with the irradiation of $1000W/m^2$.

The second set of simulations show the closed-loop TS-Fuzzy controller. Figure 13(a) shows the battery state of charging (SOC %) increases from $t=0s$ to $1.5s$. The SOC of the battery is reduced from $1.5s$, the battery current i.e. I_{bat} is reversed in direction and the battery voltage V_{bat} is given a step change from 52 volts to 51 volts as shown in Figures 13(b) and 13(c). Therefore, the BMS starts.

Here, performance parameters of different Controllers are illustrated in Table 5.

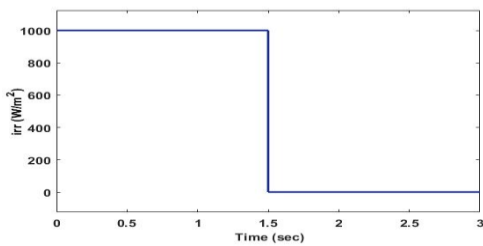


(d)

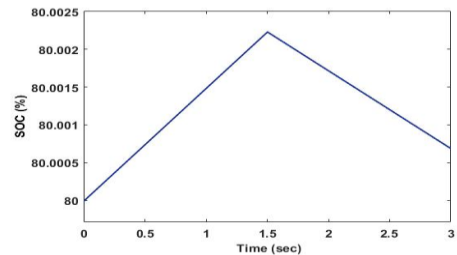


(e)

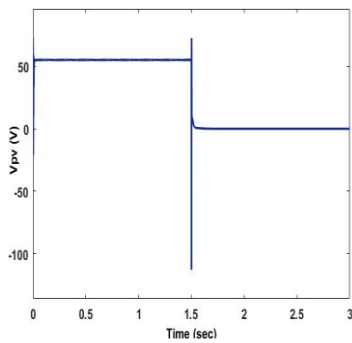
Figure 12. MATLAB simulation results of (a) irradiance, (b) output voltage, (c) current, (d) DC Bus voltage and (e) output power of PV system



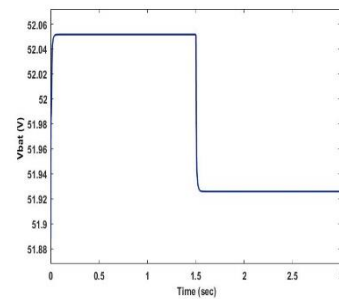
(a)



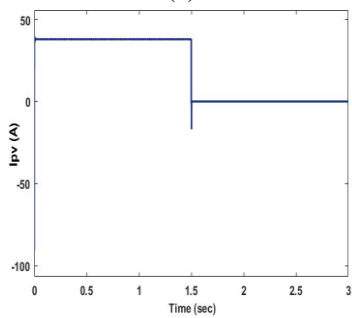
(a)



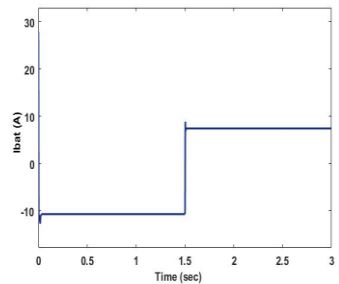
(b)



(b)



(c)



(c)

Figure 13. MATLAB simulation results of TS-Fuzzy controller (a) SOC (%) (b) V_{bat} (V) (c) I_{bat} (A)

TABLE 5. Performance parameters of different controllers

Controller		Ref [13]	Proposed TS-Fuzzy
I_{bat}	Overshoot(s)	0.05	0.002
	Undershoot(s)	0.55	0.035
Load Current	Overshoot(s)	0.4	0.002
	Undershoot(s)	0.43	0.003
Settling Time		61s	13.682ms

8. CONCLUSION

The proposed energy management system proves better performance with TS-Fuzzy controller than PI controller. Due to the advantage of less overshoot, rise time and fast dynamic response the TS-Fuzzy controller is preferred. The battery management system is used to charge and discharge the battery according to the generated power of the system. This is verified using performance parameter of the controllers. Two controller schemes PI and TS-Fuzzy have been simulated in MATLAB/SIMULINK environment and at RT-LAB. The results obtained are analyzed and performance have been compared to identify the best performer in similar conditions.

9. REFERENCES

- Majid, M., "Renewable energy for sustainable development in india: Current status, future prospects, challenges, employment, and investment opportunities", *Energy, Sustainability and Society*, Vol. 10, No. 1, (2020), 1-36. doi: 10.1186/s13705-019-0232-1.
- Faranda, R., Leva, S. and Maugeri, V., "Mppt techniques for pv systems: Energetic and cost comparison", in 2008 IEEE Power and Energy Society General Meeting-Conversion and Delivery of Electrical Energy in the 21st Century, IEEE., (2008), 1-6.
- Berrera, M., Dolara, A., Faranda, R. and Leva, S., "Experimental test of seven widely-adopted mppt algorithms", in 2009 IEEE Bucharest PowerTech, IEEE., (2009), 1-8.
- Liu, F., Duan, S., Liu, F., Liu, B. and Kang, Y., "A variable step size inc mppt method for pv systems", *IEEE Transactions on Industrial Electronics*, Vol. 55, No. 7, (2008), 2622-2628.
- Esrarn, T. and Chapman, P.L., "Comparison of photovoltaic array maximum power point tracking techniques", *IEEE Transactions on Energy Conversion*, Vol. 22, No. 2, (2007), 439-449. <http://dx.doi.org/10.1109/TEC.2006.874230>
- Eltamaly, A.M., Performance of mppt techniques of photovoltaic systems under normal and partial shading conditions, in Advances in renewable energies and power technologies. 2018, Elsevier.115-161.
- Kamal, N.A. and Ibrahim, A.M., "Conventional, intelligent, and fractional-order control method for maximum power point tracking of a photovoltaic system: A review", *Fractional Order Systems*, (2018), 603-671. <http://dx.doi.org/10.1016/B978-0-12-816152-4.00020-0>
- Zhang, K., "Control simulation and experimental verification of maximum power point tracking based on rt-lab", *International Journal of Engineering, Transactions A: Basic* Vol. 29, No. 10, (2016), 1372-1379. <http://dx.doi.org/10.5829/idosi.ije.2016.29.10a.07>
- Samadi, M.F. and Saif, M., "State-space modeling and observer design of li-ion batteries using takagi-sugeno fuzzy system", *IEEE Transactions on Control Systems Technology*, Vol. 25, No. 1, (2016), 301-308. <http://dx.doi.org/10.1109/TCST.2016.2549270>
- Samadi, M.F. and Saif, M., "Takagi-sugeno fuzzy model identification of li-ion battery systems", in 2014 World Automation Congress (WAC), IEEE., (2014), 421-426.
- Al Alahmadi, A.A., Belkhier, Y., Ullah, N., Abeida, H., Soliman, M.S., Khraisat, Y.S.H. and Alharbi, Y.M., "Hybrid wind/pv/battery energy management-based intelligent non-integer control for smart dc-microgrid of smart university", *IEEE Access*, Vol. 9, (2021), 98948-98961. <http://dx.doi.org/10.1109/ACCESS.2021.3095973>
- Subha, S. and Nagalakshmi, S., "Design of anfis controller for intelligent energy management in smart grid applications", *Journal of Ambient Intelligence and Humanized Computing*, Vol. 12, No. 6, (2021), 6117-6127. <https://doi.org/10.1007/s12652-022-04177-1>
- Cabrane, Z., Kim, J., Yoo, K. and Ouassaid, M., "Hess-based photovoltaic/batteries/supercapacitors: Energy management strategy and dc bus voltage stabilization", *Solar Energy*, Vol. 216, (2021), 551-563. <https://doi.org/10.1016/j.solener.2021.01.048>
- Parise, G., Martirano, L., Kermani, M. and Kermani, M., "Designing a power control strategy in a microgrid using pid/fuzzy controller based on battery energy storage", in 2017 IEEE International Conference on Environment and Electrical Engineering and 2017 IEEE Industrial and Commercial Power Systems Europe (EEEIC/I&CPS Europe), IEEE., (2017), 1-5.
- Pattanaik, P., "Boost converter based on photovoltaic energy system", *International Journal of Innovative Technology and Exploring Engineering*, Vol. 8, No. 11S, (2019).
- Awda, L., KHALAF, Y. and Salih, S., "Analysis of temperature effect on a crystalline silicon photovoltaic module performance", *International Journal of Engineering, Transactions B: Applications*, Vol. 29, No. 5, (2016), 722-727. <http://dx.doi.org/10.5829/idosi.ije.2016.29.05b.17>
- Verma, A.K., Singh, B. and Kaushik, S., "An isolated solar power generation using boost converter and boost inverter", *International Journal of Engineering and Information Technology*, Vol. 2, No. 2, (2010), 101-108.
- Femia, N., Petrone, G., Spagnuolo, G. and Vitelli, M., "Optimization of perturb and observe maximum power point tracking method", *IEEE Transactions on Power Electronics*, Vol. 20, No. 4, (2005), 963-973. <http://dx.doi.org/10.1109/TPEL.2005.850975>
- Bhattacharyya, S., Puchalapalli, S. and Singh, B., "Battery management and operation of a wind-pv based microgrid", in 2020 IEEE International Conference on Computing, Power and Communication Technologies (GUCON), IEEE., (2020), 423-429.

Persian Abstract

چکیده

این مقاله یک طراحی جامع و استراتژی کنترل برای یک سیستم ذخیره انرژی فتوولتائیک (PV) ارائه می‌کند. این سیستم شامل یک سیستم فتوولتائیک ۲ کیلوواتی، دو مدار مبدل، یک بار مقاومتی ۶ اهم و یک ذخیره‌سازی باتری لیتیوم یونی است که با باس DC یکپارچه شده است که برق ثابتی را به بار مقاومتی اعمال می‌کند. این طرح دو توپولوژی مبدل را ارائه می‌دهد، یکی مبدل تقویت کننده و دیگری مبدل دو طرفه DC/DC. مبدل تقویت کننده مستقیماً به صورت سری به آرایه PV متصل می‌شود در حالی که مبدل دو طرفه DC/DC (BDC) به باتری متصل است. مبدل تقویت کننده برای تنظیم حداکثر ردیابی نقطه توان (MPPT) آرایه PV استفاده می‌شود. کنترل حلقه بسته کنترل کننده دو طرفه با کنترلر Takagi-Sugeno Fuzzy (TS-Fuzzy) برای تنظیم جریان شارژ و تخلیه باتری اجرا می‌شود. طرح پیشنهادی تثبیت خوبی در ولتاژ باس DC فراهم می‌کند. نتایج شبیه‌سازی طرح‌واره کنترل پیشنهادی تحت MATLAB/Simulink ارائه شده و با کنترل کننده انتگرال متناسب (PI) مقایسه می‌شود. نتایج شبیه‌سازی به دست آمده از MATLAB در شبیه‌ساز دیجیتالی واقعی (RTDS) تأیید می‌شوند.
